Supplementary figures

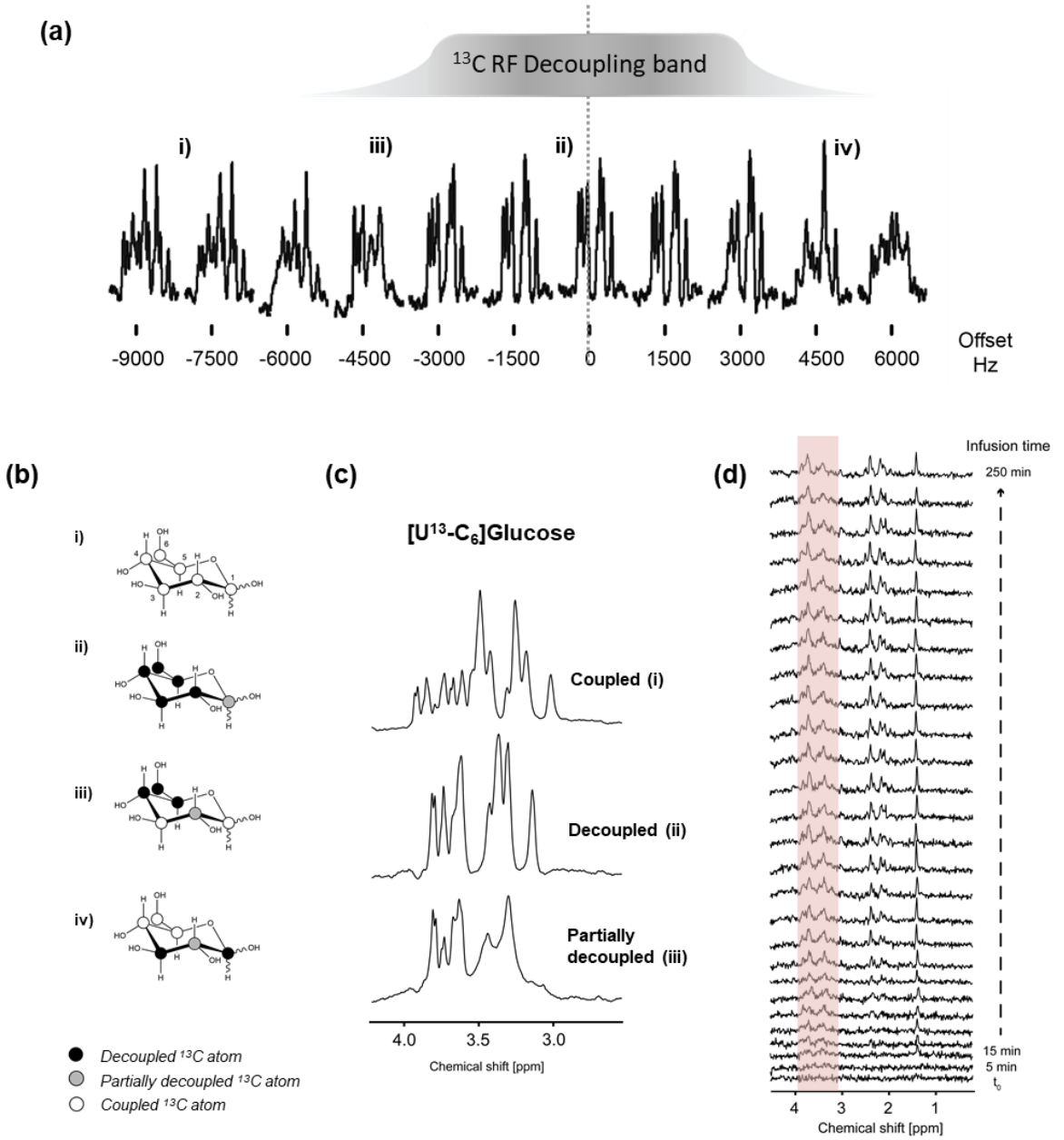

Supplementary Figure 1

^{1}H-[^{13}C]-MRS spectra of [U-^{13}C$_6$]Glc with distinct decoupling efficiencies and dynamic spectra accumulation of mouse hippocampus

(a) Example of [U-^{13}C$_6$]Glc spectral patterns with three distinct decoupling efficiencies. The shape of glucose signal varies with the frequency offset of the ^{1}H-^{13}C decoupling pulse bandwidth. **i)** fully coupled glucose, **ii)** fully decoupled glucose, **iii)** partially decoupled glucose in the ascending slope of the decoupling pulse and **iv)** partially decoupled glucose in the descending slope of the decoupling pulse. (b) [U-^{13}C$_6$]Glc carbon positions associated with the observed coupling in (a). (c) Glucose resonances used in the basis set to fit the edited spectra. (d) Typical timeline of the edited spectra over the course of [U-^{13}C$_6$]Glc infusion with a time resolution of 10min. The location of glucose in the spectra is highlighted in the shaded red area.

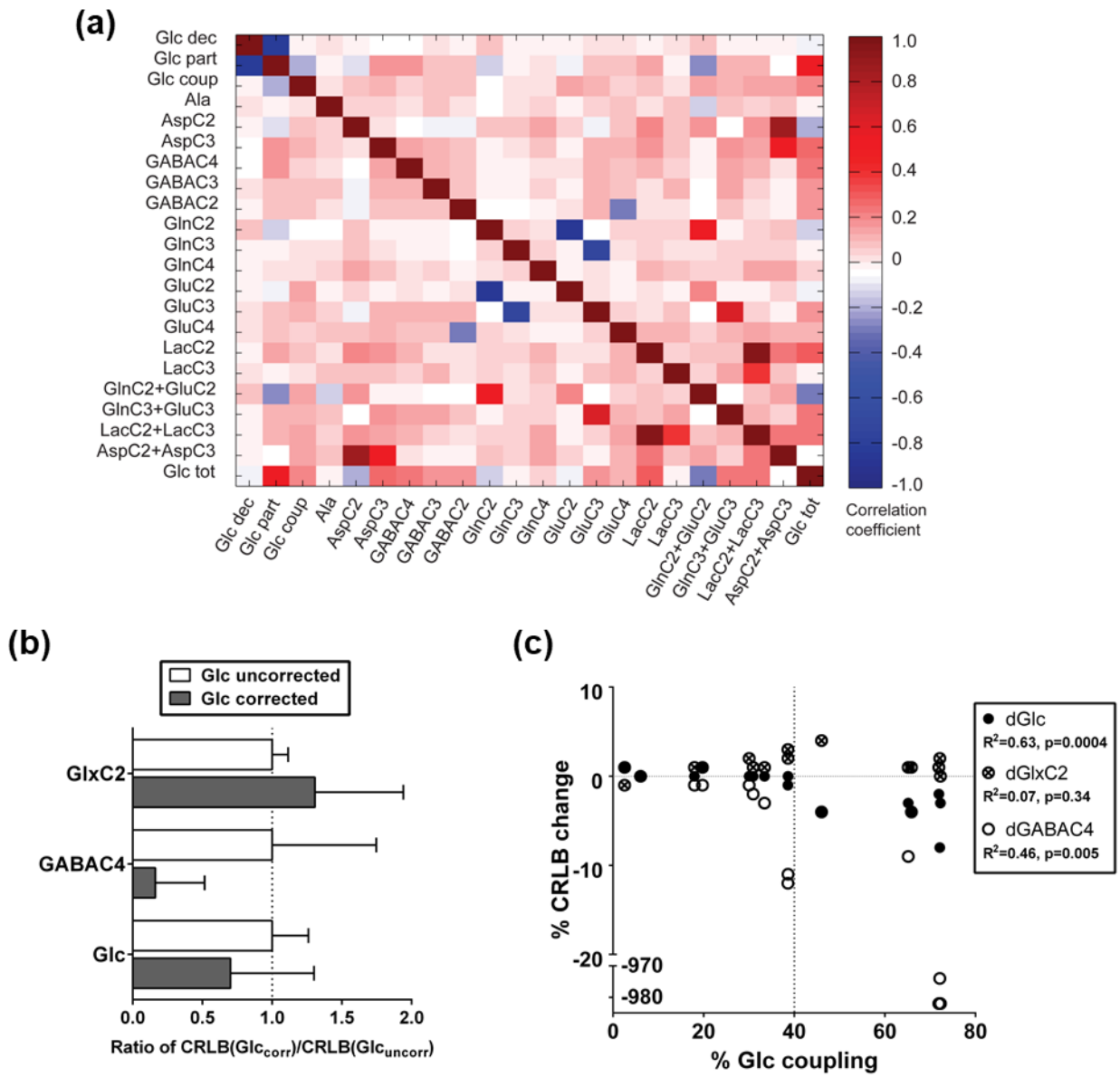

Supplementary Figure 2

Fitting improvements with a basis set corrected for glucose ^{1}H-^{13}C coupling

(a) Correlation coefficients averaged over all animals between the different fitted components of the basis set after LCModel analysis in the edited spectra. (b) Relative Cramér-Rao Lower Bound (CRLB) value using an uncorrected or corrected basis set for glucose decoupling. (c) Relation between CRLB improvement and the estimated decoupling efficiency. The corrected basis set reduced significantly the CRLB values of Glc and GABAC4 when ^{1}H-^{13}C coupling of glucose was strong.

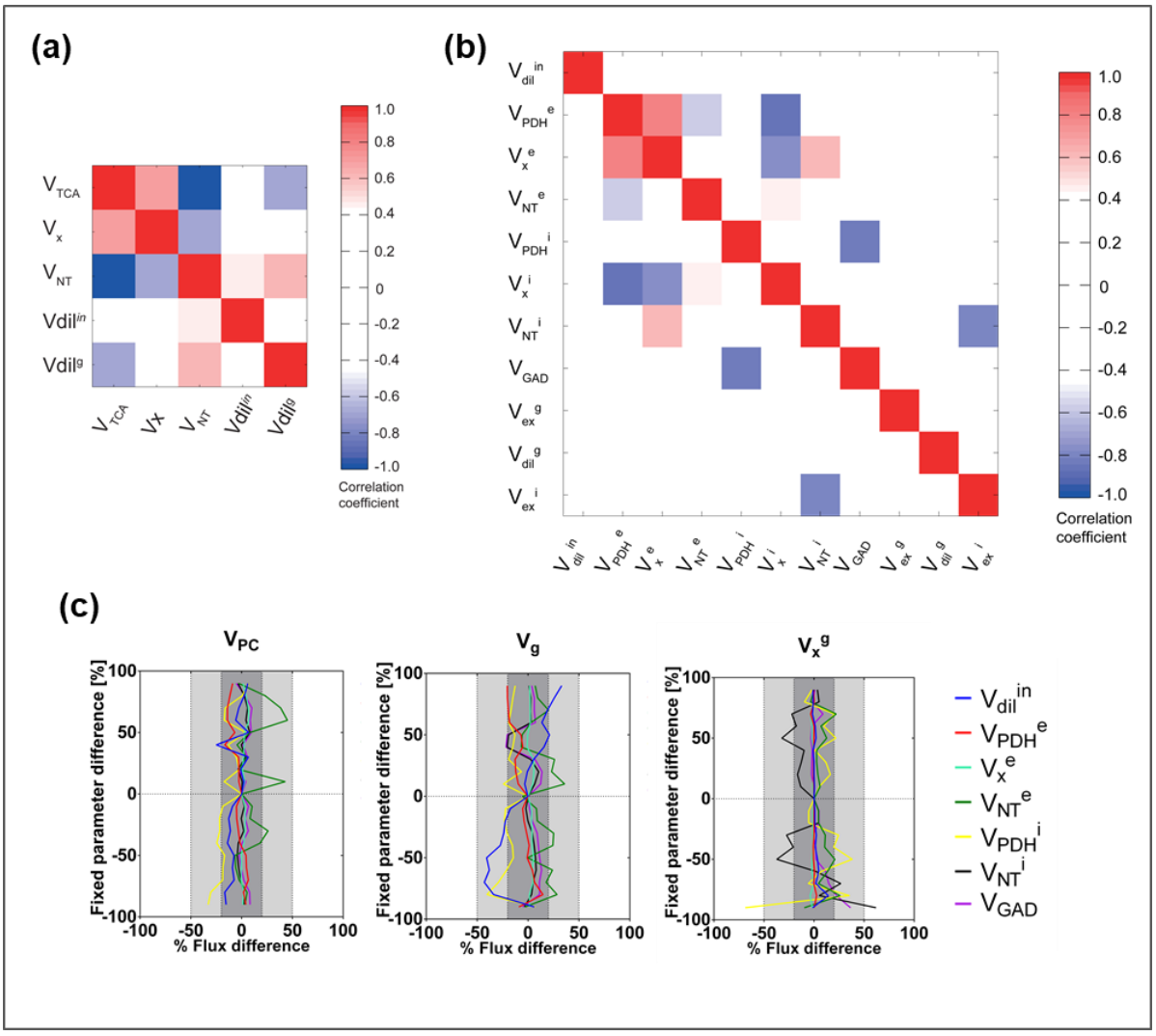

Supplementary Figure 3

Quality assessment of the 1-compartment and pseudo 3-compartment models of hippocampus metabolism

Correlation matrices of all derived fluxes obtained from the Monte-Carlo simulations with (a) a 1-compartment model and (b) a pseudo 3-compartment model. (c) Dependency of the flux estimations with the values chosen for the fixed glial parameters in the 3-compartment model: Pyruvate carboxylase (V_{PC}), glial TCA cycle (V_g) and glial transmitochondrial flux (V_x^g). Estimated fluxes included: Pyruvate dehydrogenase activity (V_{PDH}), tricarboxylic acid cycle (V_{TCA}), an influx from blood lactate (V_{dil}^{in}) and a dilution flux from blood acetate (V_{dil}^g), a transmitochondrial flux (V_x), a neurotransmission flux (V_{NT}), glutamate decarboxylase activity (V_{GAD}), and two exchange fluxes between two glial Gln or two GABA pools (V_{ex}^g and V_{ex}^i).

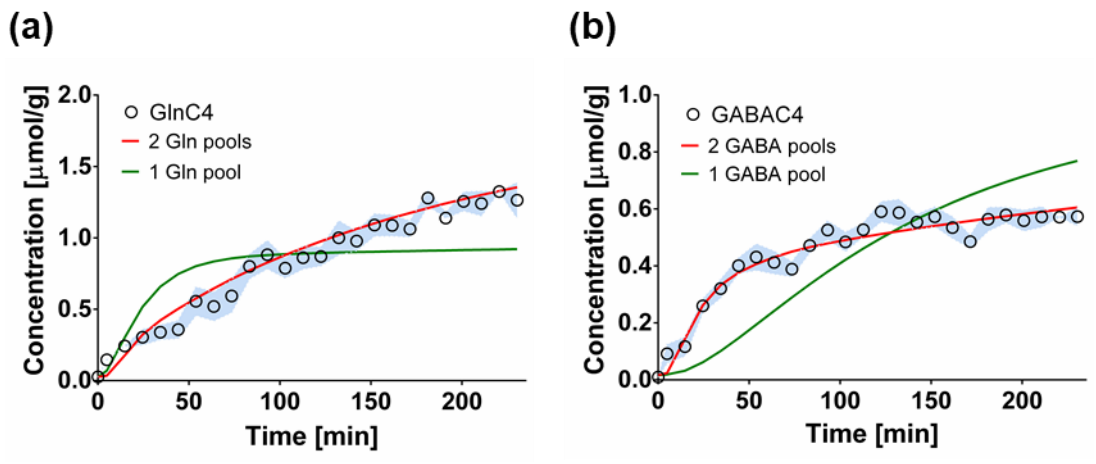

Supplementary Figure 4

Improvement of fitting quality upon addition of a second metabolite pool

(a) Effect of the addition of a second glutamine pool in a pseudo 3-compartment model. (b) Effect of the addition of a second GABA pool in a pseudo 3-compartment model. Overall, the goodness-of-fit of the whole data set improved from a 1-Gln pool model (R^2=0.976) and 1-GABA pool model (R^2=0.978) as compared to the 2-pools model (R^2=0.980).

Supplementary information on the mathematical modeling

The mathematical description of the model was adapted from previously published models[1,2]. Main differences arise from the utilization of uniformly labeled glucose and the use of brain glucose as input function, which was a main development described in this study. We propose two different models which are suitable for modeling of brain metabolism upon infusion of [U^{13}-C$_6$]glucose. Both models assume the metabolic pool sizes to be constant over the time of the infusion and were obtained from the real-time concentrations measured from the ^{1}H-MRS neurochemical profile.

1-Compartment Model

Mass-balance equations and isotope balance equations reflect the model presented in figure 4A under metabolic steady state condition. The assumptions that have been made throughout the model are described below.

Mass balance

The net amount of pyruvate oxidized by the pyruvate dehydrogenase (PDH) corresponds to the pyruvate synthesis from glycolysis, also known as the cerebral metabolic rate of glucose (CMR_g), added to the net brain lactate influx (${V_{dil}}^{in} - {V_{dil}}^{out}$).

$$V_{PDH} = 2 \cdot CMR_g + {V_{dil}}^{in} - {V_{dil}}^{out} = V_{TCA}$$

Glycolytic activity was set at CMR_g= 0.61 µmol/g/min as calculated from PET measurements in a same voxel.

Blood lactate relation

A difference in glucose consumption from glycolysis (CMR_g) and oxidation ($CMR_g(ox)$) in the mitochondria is a well-established phenomenon, which occurs during rest but mainly during neuronal activation. For instance, Patel et al.[3] found that the ratio of CMR_g over $CMR_g(ox)$ was around 1.5:1 after bicuculline-induced intense neuronal activity compared to a 1:1 ratio in controls. The resulting lactate accumulation is generally thought to be released in the blood or used internally for non-oxidative purpose. Due to the use of isoflurane anesthesia leading to possibly low neuronal activity and associated lactate dynamics, we did not assume any direct relationship between CMR_g and $CMR_g(ox)$. Rather, we propose the lactate kinetics to be defined by the measured plasma values (FE and concentration) and driven by a concentration gradient. We assumed a linear relation of brain lactate (Lac_{brain}) with plasma lactate levels (Lac_{blood}) as described in Boumezbeur et al.[4], which allowed us to predict the relation between lactate influx and efflux from the brain. Lac_{brain} was determined as the averaged concentration measured with MRS in the hippocampal voxel over the time of infusion and Lac_{blood} was set to the plasma value obtained from plasma measurements after the scan.

$${V_{dil}}^{out} = {V_{dil}}^{in} \frac{Lac_{brain}}{Lac_{blood}}$$

Blood lactate and acetate values

Because labeling of blood metabolites occurs through utilization of glucose mainly in other organs than the brain, we included the contribution of plasma lactate and acetate ^{13}C-labeling. In a separate experiment with animals

infused with [U-$^{13}C_6$]Glc outside of the scanner, we analyzed the relative labeling of glucose, lactate and acetate by performing a 3 time-point blood sampling (Fig 3(b)). Results indicated a relative steady-state of lactate FE of 0.5 with a slightly slower labeling slope than in the brain. Acetate labeling occurred more slowly and did not reach a steady state in our experimental time-frame. As a result, we used an interpolation of blood lactate and acetate data with a final value of 0.5 for both fractional enrichments (at t_4=250 min) as observed in Duarte et al[2].

$$\frac{Lac_3(t=250)_{Blood}}{Lac_{Blood}} = 0.5 \qquad \frac{Acetate_2(t=250)_{Blood}}{Acetate_{Blood}} = 0.5$$

Lactate-pyruvate fast exchange

Pyruvate FE can be considered equal to Lactate FE in the brain due to fast exchange occurring with lactate dehydrogenase (LDH) activity[5,6].

$$\frac{Pyr_3(t)}{Pyr} = \frac{Lac_3(t)}{Lac}$$

Uniformly labeling of glucose considerations

The use of uniformly labeled glucose allows a set of possible assumptions and simplifications in the model. The absence of a differential labeling arising from pyruvate carboxylation in glial cells typically observed with [1,6-$^{13}C_2$]Glc leads to a similar enrichment profile of several C2 and C3 positions of TCA cycle intermediates and thus metabolites in direct exchange with it. Typically: OAAC3(t)=OAAC2(t), OG3(t)=OG2(t), AspC3(t)=AspC2(t), GluC3(t)=GluC2(t) and GlnC3(t)=GlnC2(t).

$$\frac{Asp_3(t)}{Asp} = \frac{Asp_2(t)}{Asp} \leftrightarrow \frac{OAA_3(t)}{OAA} = \frac{OAA_2(t)}{OAA}$$

Set of differential equations

The set of differential equations used in the 1-compartment model is shown below. The small intermediates (OAA, OG and AcCoA) pool sizes were all approximated at 0.1 µmol/g as reported in Duarte et al.[2]. The mathematical model used the brain glucose fractional enrichment as input function (IF). The estimated fluxes were: the tricarboxylic acid cycle flux ($V_{TCA} = 2 \cdot CMR_g(ox)$), transmitochondrial flux (V_x), a dilution flux from plasma lactate (${V_{dil}}^{in}$), the neurotransmission or Gln/Glu cycle flux (V_{NT}), and a dilution factor arising from mitochondrial oxidation of ketone bodies, fatty acids or acetate (${V_{dil}}^{g}$).

Glu C4: $$\frac{dGlu_4}{dt} = V_x \cdot \frac{OG_4(t)}{OG} + V_{NT} \cdot \frac{Gln_4(t)}{Gln} - (V_x + V_{NT}) \cdot \frac{Glu_4(t)}{Glu}$$

Glu C3: $$\frac{dGlu_3}{dt} = V_x \cdot \frac{OG_3(t)}{OG} + V_{NT} \cdot \frac{Gln_3(t)}{Gln} - (V_x + V_{NT}) \cdot \frac{Glu_3(t)}{Glu}$$

Gln C4: $$\frac{dGln_4}{dt} = V_{NT} \cdot \frac{Glu_4(t)}{Glu} - V_{NT} \cdot \frac{Gln_4(t)}{Gln}$$

Gln C3: $$\frac{dGln_3}{dt} = V_{NT} \cdot \frac{Glu_3(t)}{Glu} - V_{NT} \cdot \frac{Gln_3(t)}{Gln}$$

Asp C3: $$\frac{dAsp_3}{dt} = V_x \cdot \frac{OAA_3(t)}{OAA} - V_x \cdot \frac{Asp_3(t)}{Asp}$$

Asp C2: $$\frac{dAsp_2}{dt} = V_x \cdot \frac{OAA_2(t)}{OAA} - V_x \cdot \frac{Asp_2(t)}{Asp}$$

OG C4: $$\frac{dOG_4}{dt} = V_{TCA} \cdot \frac{AcCoA_2(t)}{AcCoA} + V_x \cdot \frac{Glu_4(t)}{Glu} - (V_x + V_{TCA}) \cdot \frac{OG_4(t)}{OG}$$

OG C3: $\frac{dOG_3}{dt} = V_{TCA} \cdot \frac{OAA_2(t)}{OAA} + V_x \cdot \frac{Glu_3(t)}{Glu} - (V_x + V_{TCA}) \cdot \frac{OG_3(t)}{OG}$

OAA C3: $\frac{dOAA_3}{dt} = \frac{1}{2} \cdot V_{TCA} \cdot \frac{OG_4(t)}{OG} + \frac{1}{2} \cdot V_{TCA} \cdot \frac{OG_3(t)}{OG} + V_x \cdot \frac{Asp_3(t)}{Asp} - (V_x + V_{TCA}) \cdot \frac{OAA_3(t)}{OAA}$

OAA C2: $\frac{dOAA_2}{dt} = \frac{1}{2} \cdot V_{TCA} \cdot \frac{OG_4(t)}{OG} + \frac{1}{2} \cdot V_{TCA} \cdot \frac{OG_3(t)}{OG} + V_x \cdot \frac{Asp_2(t)}{Asp} - (V_x + V_{TCA}) \cdot \frac{OAA_2(t)}{OAA}$

Lac C3: $\frac{dLac_3}{dt} = 2 \cdot CMR_g \cdot IF + {V_{dil}}^{in} \cdot \frac{Lac_3(t)_{Blood}}{Lac_{Blood}} - (V_{TCA} + {V_{dil}}^{out}) \frac{Lac_3(t)}{Lac}$

AcCoA C2: $\frac{dAcCoA_2}{dt} = V_{TCA} \cdot \frac{Pyr_3(t)}{Pyr} + {V_{dil}}^{g} \cdot \frac{Acetate_2(t)_{Blood}}{Acetate_{Blood}} - (V_{TCA} + {V_{dil}}^{g}) \cdot \frac{AcCoA_2(t)}{AcCoA}$

Pseudo 3-Compartment Model

Brain metabolism is highly compartmentalized and therefore ideally requires a distinction between the different cellular compartments present in the brain for an accurate mathematical modeling[7]. Typically, brain compartments are generally segregated into neuronal and astrocytic metabolism. Excitatory neurons release neurotransmitter glutamate in the synaptic cleft, which is taken up by astrocytes and recycled back. This process is known as the Glu-Gln cycle, or neurotransmission rate, as it is based on the astroglial ability to rapidly convert the glutamate taken up and converted to glutamine via the enzyme glutamine synthetase (GS) and shuttle it back into neurons[8]. This cycle exists for GABA in inhibitory neurons as well, with the main difference that GABA is recycled via the GABA shunt after release by inhibitory neurons. This pathway consists in the transformation of GABA into succinate through the action of GABA transaminase, which is re-incorporated into the TCA cycle[9]. Another specificity of glial metabolism is the anaplerotic reactions taking place through the action of pyruvate carboxylase (PC), which converts pyruvate into oxaloacetate, which feeds the TCA cycle. This reaction is central for the distinction between neurons and astrocyte metabolism. The [3-^{13}C]pyruvate formed from [1,6-$^{13}C_2$]glucose produces a specific ^{13}C-labeling dilution on position C2 of the glutamate and glutamine measured upon exchange with TCA cycle intermediates. This dilution effect is not produced with [U-$^{13}C_6$]glucose rendering the assessment of glial metabolism impossible. Therefore, we have fixed all the glial parameters based on values from the literature. The model proposed here is an extended version of the aforementioned 1-compartment model, with several additions adapted from Duarte et al.[2]. A scheme of metabolic fluxes and compartments is shown in Figure 1(b).

Uniformly labeling of glucose considerations

As for the 1-compartment model description, a major simplification was made to reduce the number of equations to be used. Mainly, labeling of AspC3 was set equal to AspC2, GluC3 set equal to GluC2 and GlnC3 set equal to GlnC2.

$$\frac{Asp_3(t)}{Asp} = \frac{Asp_2(t)}{Asp} \qquad \frac{OAA_3(t)}{OAA} = \frac{OAA_2(t)}{OAA}$$

As an attempt to improve the amount of available data to gain precision in the modeling, we also included a separation of GluC2 and GlnC2. As we were not able to separate these two resonances in the fitting process but only had access to GlxC2, we extracted the relative concentrations based on the measured GlnC3 and GluC3 results. This correction process is only possible due to the absence of ^{13}C-dilution from arising from PC activity:

$$\frac{Glu_3(t)}{Glx_3(t)} = \frac{Glu_2(t)}{Glx_2(t)} \qquad \frac{Gln_3(t)}{Glx_3(t)} = \frac{Gln_2(t)}{Glx_2(t)}$$

Pool sizes

The metabolic pool sizes of the small TCA intermediates pools were all fixed at 0.1 µmol/g in all three compartments[2]: glia (^{g}), excitatory neurons (^{e}) and inhibitory neurons (^{i}).

$$AcCoA^g = OG^e = OG^i = OG^g = OAA^e = OAA^i = OAA^g = 0.1 \text{ µmol/g}$$

The other cell-specific metabolic pool sizes were comparable as in Duarte et al[2]:

80% of all glutamate is in excitatory neurons, the rest is distributed equally

$$Glu^e = 0.8 \cdot (Glu^e + Glu^i + Glu^g)$$

$$Glu^i = 0.1 \cdot (Glu^e + Glu^i + Glu^g)$$

$$Glu^g = 0.1 \cdot (Glu^e + Glu^i + Glu^g)$$

80% of all aspartate is in excitatory neurons, the rest is distributed equally

$$Asp^e = 0.8 \cdot (Asp^e + Asp^i + Asp^g)$$

$$Asp^i = 0.1 \cdot (Asp^e + Asp^i + Asp^g)$$

$$Asp^g = 0.1 \cdot (Asp^e + Asp^i + Asp^g)$$

80% of all glutamine is glial, the rest is distributed equally

$$Gln^g = 0.8 \cdot (Gln^e + Gln^i + Gln^g)$$

$$Gln^i = 0.1 \cdot (Gln^e + Gln^i + Gln^g)$$

$$Gln^e = 0.1 \cdot (Gln^e + Gln^i + Gln^g)$$

90% of all GABA is in inhibitory neurons, the rest is in glial cells only

$$GABA^i = 0.9 \cdot (GABA^i + GABA^g)$$

$$GABA^g = 0.1 \cdot (GABA^i + GABA^g)$$

Lactate dynamics

As for the 1-compartment model, the following relationship was used for blood lactate dynamics. Blood lactate and acetate enrichment values were approximated as in the 1-compartment model using a linear interpolation of measured fractional enrichments (FE = 0.5 at t_4 = 250 min).

$$V_{dil}{}^{out} = V_{dil}{}^{in} \frac{Lac_{brain}}{Lac_{blood}} \qquad \frac{Lac_3(t=250)_{Blood}}{Lac_{Blood}} = 0.5 \qquad \frac{Acetate_2(t=250)_{Blood}}{Acetate_{Blood}} = 0.5 \qquad \frac{Pyr_3(t)}{Pyr} = \frac{Lac_3(t)}{Lac}$$

Mass balance

The amount of glucose oxidized entering the TCA cycle is defined as the oxidative cerebral metabolic rate of glucose $CMR_g(ox)$. A factor 2 is added to consider that 1 mole of glucose is converted to 2 moles of pyruvate.

$$2 \cdot CMR_g(ox) = 2 \cdot CMR_g + V_{dil}{}^{in} - V_{dil}{}^{out}$$

Glycolytic activity was set at CMR_g= 0.61 µmol/g/min as calculated from PET measurements in a same voxel. The different cellular contributions to the total TCA cycle activity were similar as described in Duarte et al[2]. TCA cycle activity of excitatory neurons is based mainly on PDH activity, while an extra contribution of GABA shunt is added in inhibitory neurons. Similarly, glial TCA cycle includes a contribution from glial GABA shunt (V_{shunt}) together with the extra amount of oxaloacetate produced from pyruvate carboxylation which must be oxidized to maintain anaplerosis (V_{PC}).

$$V_{TCA}{}^e = V_{PDH}{}^e$$

$$V_{TCA}{}^i = V_{PDH}{}^i + V_{shunt}{}^i$$

$$V_{TCA}{}^{g} = V_g + V_{PC} + V_{shunt}{}^{g}$$

The total rate of glucose oxidation entering the TCA cycle at steady state is then equal to the sum of the cell-specific TCA components and the proportion of glucose used for pyruvate carboxylation.

$$CMR_{g(ox)} = (V_{TCA}{}^{e} + V_{TCA}{}^{i} + V_{TCA}{}^{g} + V_{PC})/2$$

GABA recycling V_{shunt} in inhibitory neurons equals the rate of GABA synthesis from glutamate decarboxylation (V_{GAD}) minus the amount which is taken up by astrocytes ($V_{NT}{}^{i}$).

$$V_{shunt}{}^{i} = V_{GAD} - V_{NT}{}^{i}$$

All the GABA entering the glial compartment is considered to be recycled through the glial GABA shunt.

$$V_{shunt}{}^{g} = V_{NT}{}^{i}$$

The synthesis of glutamine in astrocytes corresponds to the amount of glutamate taken up from excitatory neurotransmission summed with the anaplerosis induced by the amount of oxaloacetate produced from GABA recycling and PC activity

$$V_{GS} = V_{NT}{}^{e} + V_{shunt}{}^{g} + V_{PC} = V_{NT}{}^{e} + V_{NT}{}^{i} + V_{eff}$$

Fixed parameters

Pyruvate carboxylase activity (V_{PC}), glial TCA cycle (V_g) and glial transmitochondrial flux ($V_x{}^{g}$) were fixed to known values of mice from the literature[10].

Astrocyte metabolism

$$V_{PC} = 0.04 \text{ µmol/g/min}$$

$$V_g = 0.16 \text{ µmol/g/min}$$

$$V_x{}^{g} = V_g$$

Mainly, pyruvate carboxylation flux was set to V_{pc} = 0.04 µmol/g/min and equal to a net efflux of glutamine from the brain (V_{eff}). Glial V_g = 0.16 µmol/g/min and $V_x = V_g$.

Set of differential equations

Mass-balance equations and isotope balance equations reflect the model presented in Figure 1(b) under metabolic steady state condition.

Lac C3: $$\frac{dLac_3}{dt} = 2 \cdot CMR_{Glc} \cdot IF + V_{dil}{}^{in} \cdot \frac{Lac_3(t)_{Blood}}{Lac_{Blood}} - (V_{TCA} + V_{dil}{}^{out}) \frac{Lac_3(t)}{Lac}$$

Excitatory Neuron

Glu C4: $$\frac{dGlu_4{}^{e}}{dt} = V_x{}^{e} \cdot \frac{OG_4{}^{e}(t)}{OG^{e}} + V_{NT}{}^{e} \cdot \frac{Gln_4{}^{e}(t)}{Gln^{e}} - (V_x{}^{e} + V_{NT}{}^{e}) \cdot \frac{Glu_4{}^{e}(t)}{Glu^{e}}$$

Glu C3: $$\frac{dGlu_3{}^e}{dt} = V_x{}^e \cdot \frac{OG_3{}^e(t)}{OG^e} + V_{NT}{}^e \cdot \frac{Gln_3{}^e(t)}{Gln^e} - (V_x{}^e + V_{NT}{}^e) \cdot \frac{Glu_3{}^e(t)}{Glu^e}$$

Glu C2: $$\frac{dGlu_2{}^e}{dt} = V_x{}^e \cdot \frac{OG_2{}^e(t)}{OG^e} + V_{NT}{}^e \cdot \frac{Gln_2{}^e(t)}{Gln^e} - (V_x{}^e + V_{NT}{}^e) \cdot \frac{Glu_2{}^e(t)}{Glu^e}$$

Gln C4: $$\frac{dGln_4{}^e}{dt} = V_{NT}{}^e \cdot \frac{Gln_4{}^g(t)}{Glu^e} - V_{NT}{}^e \cdot \frac{Gln_4{}^e(t)}{Gln^e}$$

Gln C3: $$\frac{dGln_3{}^e}{dt} = V_{NT}{}^e \cdot \frac{Gln_3{}^g(t)}{Glu^e} - V_{NT}{}^e \cdot \frac{Gln_3{}^e(t)}{Gln^e}$$

Gln C2: $$\frac{dGln_2{}^e}{dt} = V_{NT}{}^e \cdot \frac{Gln_2{}^g(t)}{Glu^e} - V_{NT}{}^e \cdot \frac{Gln_2{}^e(t)}{Gln^e}$$

Asp C3: $$\frac{dAsp_3{}^e}{dt} = V_x \cdot \frac{OAA_3{}^e(t)}{OAA^e} - V_x \cdot \frac{Asp_3{}^e(t)}{Asp^e}$$

Asp C2: $$\frac{dAsp_2{}^e}{dt} = V_x \cdot \frac{OAA_2{}^e(t)}{OAA^e} - V_x \cdot \frac{Asp_2{}^e(t)}{Asp^e}$$

OG C4: $$\frac{dOG_4{}^e}{dt} = V_{PDH}{}^e \cdot \frac{Pyr_3(t)}{Pyr} + V_x{}^e \cdot \frac{Glu_4{}^e(t)}{Glu^e} - (V_x{}^e + V_{PDH}{}^e) \cdot \frac{OG_4{}^e(t)}{OG^e}$$

OG C3: $$\frac{dOG_3{}^e}{dt} = V_{PDH}{}^e \cdot \frac{OAA_2{}^e(t)}{OAA^e} + V_x{}^e \cdot \frac{Glu_3{}^e(t)}{Glu^e} - (V_x{}^e + V_{PDH}{}^e) \cdot \frac{OG_3{}^e(t)}{OG^e}$$

OG C2: $$\frac{dOG_2{}^e}{dt} = V_{PDH}{}^e \cdot \frac{OAA_3{}^e(t)}{OAA^e} + V_x{}^e \cdot \frac{Glu_2{}^e(t)}{Glu^e} - (V_x{}^e + V_{PDH}{}^e) \cdot \frac{OG_2{}^e(t)}{OG^e}$$

OAA C3: $$\frac{dOAA_3{}^e}{dt} = \frac{1}{2} \cdot V_{PDH}{}^e \cdot \frac{OG_4{}^e(t)}{OG^e} + \frac{1}{2} \cdot V_{PDH}{}^e \cdot \frac{OG_3{}^e(t)}{OG^e} + V_x{}^e \cdot \frac{Asp_3{}^e(t)}{Asp^e} - (V_x{}^e + V_{PDH}{}^e) \cdot \frac{OAA_3{}^e(t)}{OAA^e}$$

OAA C2: $$\frac{dOAA_2{}^e}{dt} = \frac{1}{2} \cdot V_{PDH}{}^e \cdot \frac{OG_4{}^e(t)}{OG^e} + \frac{1}{2} \cdot V_{TCA}{}^e \cdot \frac{OG_3{}^3(t)}{OG^3} + V_x{}^e \cdot \frac{Asp_2{}^e(t)}{Asp^e} - (V_x{}^e + V_{PDH}{}^e) \cdot \frac{OAA_2{}^e(t)}{OAA^e}$$

Inhibitory Neuron

Glu C4: $$\frac{dGlu_4{}^i}{dt} = (V_x{}^i + V_{shunt}{}^i) \cdot \frac{OG_4{}^i(t)}{OG^i} + V_{NT}{}^i \cdot \frac{Gln_4{}^i(t)}{Gln^i} - (V_x{}^i + V_{GAD}) \cdot \frac{Glu_4{}^i(t)}{Glu^i}$$

Glu C3: $$\frac{dGlu_3{}^i}{dt} = (V_x{}^i + V_{shunt}{}^i) \cdot \frac{OG_3{}^i(t)}{OG^i} + V_{NT}{}^i \cdot \frac{Gln_3{}^i(t)}{Gln^i} - (V_x{}^i + V_{GAD}) \cdot \frac{Glu_3{}^i(t)}{Glu^i}$$

Glu C2: $$\frac{dGlu_2{}^i}{dt} = (V_x{}^i + V_{shunt}{}^i) \cdot \frac{OG_2{}^i(t)}{OG^i} + V_{NT}{}^i \cdot \frac{Gln_2{}^i(t)}{Gln^i} - (V_x{}^i + V_{GAD}) \cdot \frac{Glu_2{}^i(t)}{Glu^i}$$

Gln C4: $$\frac{dGln_4{}^i}{dt} = V_{NT}{}^i \cdot \frac{Gln_4{}^g(t)}{Glu^i} - V_{NT}{}^i \cdot \frac{Gln_4{}^i(t)}{Gln^i}$$

Gln C3: $$\frac{dGln_3{}^i}{dt} = V_{NT}{}^i \cdot \frac{Gln_3{}^g(t)}{Glu^i} - V_{NT}{}^i \cdot \frac{Gln_3{}^i(t)}{Gln^i}$$

Gln C2: $$\frac{dGln_2{}^i}{dt} = V_{NT}{}^i \cdot \frac{Gln_2{}^g(t)}{Glu^e} - V_{NT}{}^i \cdot \frac{Gln_2{}^i(t)}{Gln^e}$$

Asp C3: $$\frac{dAsp_3{}^i}{dt} = V_x \cdot \frac{OAA_3{}^i(t)}{OAA^i} - V_x \cdot \frac{Asp_3{}^i(t)}{Asp^i}$$

Asp C2: $$\frac{dAsp_2{}^i}{dt} = V_x \cdot \frac{OAA_2{}^i(t)}{OAA^i} - V_x \cdot \frac{Asp_2{}^i(t)}{Asp^i}$$

OG C4: $$\frac{dOG_4{}^i}{dt} = (V_{PDH}{}^i + V_{shunt}{}^i) \cdot \frac{Pyr_3(t)}{Pyr} + V_x{}^i \cdot \frac{Glu_4{}^i(t)}{Glu^i} - (V_x{}^i + V_{PDH}{}^i + V_{shunt}{}^i) \cdot \frac{OG_4{}^i(t)}{OG^i}$$

OG C3: $$\frac{dOG_3{}^i}{dt} = (V_{PDH}{}^i + V_{shunt}{}^i) \cdot \frac{OAA_2{}^i(t)}{OAA^i} + V_x{}^i \cdot \frac{Glu_3{}^i(t)}{Glu^i} - (V_x{}^i + V_{PDH}{}^i + V_{shunt}{}^i) \cdot \frac{OG_3{}^i(t)}{OG^i}$$

OG C2: $$\frac{dOG_2{}^i}{dt} = (V_{PDH}{}^i + V_{shunt}{}^i) \cdot \frac{OAA_3{}^i(t)}{OAA^i} + V_x{}^i \cdot \frac{Glu_2{}^i(t)}{Glu^i} - (V_x{}^i + V_{PDH}{}^i + V_{shunt}{}^i) \cdot \frac{OG_2{}^i(t)}{OG^e}$$

OAA C3: $\frac{dOAA_3{}^i}{dt} = \frac{1}{2} \cdot V_{PDH}{}^i \cdot \frac{OG_4{}^i(t)}{OG^i} + \frac{1}{2} \cdot V_{PDH}{}^i \cdot \frac{OG_3{}^e(t)}{OG^e} + \frac{1}{2} \cdot V_{shunt}{}^i \cdot \frac{GABA_2{}^i(t)}{GABA^i} + \frac{1}{2} \cdot V_{shunt}{}^i \cdot \frac{GABA_3{}^i(t)}{GABA^i} + V_x{}^i \cdot \frac{Asp_3{}^i(t)}{Asp^i} - (V_x{}^i + V_{PDH}{}^i + V_{shunt}{}^i) \cdot \frac{OAA_3{}^i(t)}{OAA^i}$

OAA C2: $\frac{dOAA_2{}^i}{dt} = \frac{1}{2} \cdot V_{PDH}{}^i \cdot \frac{OG_4{}^i(t)}{OG^i} + \frac{1}{2} \cdot V_{PDH}{}^i \cdot \frac{OG_3{}^e(t)}{OG^e} + \frac{1}{2} \cdot V_{shunt}{}^i \cdot \frac{GABA_2{}^i(t)}{GABA^i} + \frac{1}{2} \cdot V_{shunt}{}^i \cdot \frac{GABA_3{}^i(t)}{GABA^i} + V_x{}^i \cdot \frac{Asp_2{}^i(t)}{Asp^i} - (V_x{}^i + V_{PDH}{}^i + V_{shunt}{}^i) \cdot \frac{OAA_2{}^i(t)}{OAA^i}$

GABA C2: $\frac{dGABA_2{}^i}{dt} = V_{GAD} \cdot \frac{Glu_4{}^i(t)}{Glu^i} - (V_{NT}{}^i + V_{shunt}{}^i) \cdot \frac{GABA_2{}^i(t)}{GABA^i}$

GABA C3: $\frac{dGABA_3{}^i}{dt} = V_{GAD} \cdot \frac{Glu_3{}^i(t)}{Glu^i} - (V_{NT}{}^i + V_{shunt}{}^i) \cdot \frac{GABA_3{}^i(t)}{GABA^i}$

GABA C4: $\frac{dGABA_4{}^i}{dt} = V_{GAD} \cdot \frac{Glu_2{}^i(t)}{Glu^i} - (V_{NT}{}^i + V_{shunt}{}^i) \cdot \frac{GABA_4{}^i(t)}{GABA^i}$

Glial compartment

AcCoA C2: $\frac{dAcCoA_2{}^g}{dt} = (V_g + V_{shunt}{}^g + V_{PC}) \cdot \frac{Pyr_3(t)}{Pyr} + V_{dil}{}^g \cdot \frac{Acetate_2(t)_{Blood}}{Acetate_{Blood}} - (V_g + V_{shunt}{}^g + V_{PC} + V_{dil}{}^g) \cdot \frac{AcCoA_2{}^g(t)}{AcCoA^g}$

Glu C4: $\frac{dGlu_4{}^g}{dt} = (V_x{}^g + V_{shunt}{}^g + V_{PC}) \cdot \frac{OG_4{}^g(t)}{OG^g} + V_{NT}{}^e \cdot \frac{Glu_4{}^e(t)}{Glu^e} - (V_{GS} + V_x{}^g) \cdot \frac{Glu_4{}^g(t)}{Glu^g}$

Glu C3: $\frac{dGlu_3{}^g}{dt} = (V_x{}^g + V_{shunt}{}^g + V_{PC}) \cdot \frac{OG_3{}^g(t)}{OG^g} + V_{NT}{}^e \cdot \frac{Glu_3{}^e(t)}{Glu^e} - (V_{GS} + V_x{}^g) \cdot \frac{Glu_3{}^g(t)}{Glu^g}$

Glu C2: $\frac{dGlu_2{}^g}{dt} = (V_x{}^g + V_{shunt}{}^g + V_{PC}) \cdot \frac{OG_2{}^g(t)}{OG^g} + V_{NT}{}^e \cdot \frac{Glu_2{}^e(t)}{Glu^e} - (V_{GS} + V_x{}^g) \cdot \frac{Glu_2{}^g(t)}{Glu^g}$

Gln C4: $\frac{dGln_4{}^g}{dt} = V_{GS} \cdot \frac{Glu_4{}^g(t)}{Glu^g} - (V_{NT}{}^i + V_{NT}{}^e + V_{eff}) - \frac{Gln_4{}^g(t)}{Gln^g}$

Gln C3: $\frac{dGln_3{}^g}{dt} = V_{GS} \cdot \frac{Glu_3{}^g(t)}{Glu^g} - (V_{NT}{}^i + V_{NT}{}^e + V_{eff}) - \frac{Gln_3{}^g(t)}{Gln^g}$

Gln C2: $\frac{dGln_2{}^g}{dt} = V_{GS} \cdot \frac{Glu_2{}^g(t)}{Glu^g} - (V_{NT}{}^i + V_{NT}{}^e + V_{eff}) - \frac{Gln_2{}^g(t)}{Gln^g}$

Asp C3: $\frac{dAsp_3{}^g}{dt} = V_x{}^g \cdot \frac{OAA_3{}^g(t)}{OAA^g} - V_x{}^g \cdot \frac{Asp_3{}^g(t)}{Asp^g}$

Asp C2: $\frac{dAsp_2{}^g}{dt} = V_x{}^g \cdot \frac{OAA_2{}^g(t)}{OAA^g} - V_x{}^g \cdot \frac{Asp_2{}^g(t)}{Asp^g}$

OG C4: $\frac{dOG_4{}^g}{dt} = (V_x{}^g + V_{shunt}{}^g + V_{PC}) \cdot \frac{Pyr_3(t)}{Pyr} + V_x{}^g \cdot \frac{Glu_4{}^g(t)}{Glu^g} - (V_x{}^g + V_{shunt}{}^g + V_g + V_{PC}) \cdot \frac{OG_4{}^g(t)}{OG^g}$

OG C3: $\frac{dOG_3{}^g}{dt} = (V_x{}^g + V_{shunt}{}^g + V_{PC}) \cdot \frac{OAA_2{}^g(t)}{OAA^g} + V_x{}^g \cdot \frac{Glu_3{}^g(t)}{Glu^g} - (V_x{}^g + V_{shunt}{}^g + V_g + V_{PC}) \cdot \frac{OG_3{}^g(t)}{OG^g}$

OG C2: $\frac{dOG_2{}^g}{dt} = (V_x{}^g + V_{shunt}{}^g + V_{PC}) \cdot \frac{OAA_3{}^g(t)}{OAA^g} + V_x{}^g \cdot \frac{Glu_2{}^g(t)}{Glu^g} - (V_x{}^g + V_{shunt}{}^g + V_g + V_{PC}) \cdot \frac{OG_2{}^g(t)}{OG^g}$

OAA C3: $\frac{dOAA_3{}^g}{dt} = \frac{1}{2} \cdot V_g \cdot \frac{OG_4{}^g(t)}{OG^g} + \frac{1}{2} \cdot V_g \cdot \frac{OG_3{}^g(t)}{OG^g} + \frac{1}{2} \cdot V_{shunt}{}^g \cdot \frac{GABA_2{}^g(t)}{GABA^g} + \frac{1}{2} \cdot V_{shunt}{}^g \cdot \frac{GABA_3{}^g(t)}{GABA^g} + V_{PC} \cdot \frac{Pyr_3(t)}{Pyr} + V_x{}^g \cdot \frac{Asp_3{}^g(t)}{Asp^g} - (V_x{}^g + V_{shunt}{}^g + V_g + V_{PC}) \cdot \frac{OAA_3{}^g(t)}{OAA^g}$

OAA C2: $\frac{dOAA_2{}^g}{dt} = \frac{1}{2} \cdot V_g \cdot \frac{OG_4{}^g(t)}{OG^g} + \frac{1}{2} \cdot V_g \cdot \frac{OG_3{}^g(t)}{OG^g} + \frac{1}{2} \cdot V_{shunt}{}^g \cdot \frac{GABA_2{}^g(t)}{GABA^g} + \frac{1}{2} \cdot V_{shunt}{}^g \cdot \frac{GABA_3{}^g(t)}{GABA^g} + V_{PC} \cdot \frac{Pyr_2(t)}{Pyr} + V_x{}^g \cdot \frac{Asp_2{}^g(t)}{Asp^g} - (V_x{}^g + V_{shunt}{}^g + V_g + V_{PC}) \cdot \frac{OAA_2{}^g(t)}{OAA^g}$

GABA C2: $\frac{dGABA_2{}^g}{dt} = V_{NT}{}^i \cdot \frac{GABA_2{}^i(t)}{GABA^i} - V_{shunt}{}^g \cdot \frac{GABA_2{}^g(t)}{GABA^g}$

GABA C3: $\frac{dGABA_3{}^g}{dt} = V_{NT}{}^i \cdot \frac{GABA_3{}^i(t)}{GABA^i} - V_{shunt}{}^g \cdot \frac{GABA_3{}^g(t)}{GABA^g}$

GABA C4: $\frac{dGABA_4{}^g}{dt} = V_{NT}{}^i \cdot \frac{GABA_4{}^i(t)}{GABA^i} - V_{shunt}{}^g \cdot \frac{GABA_4{}^g(t)}{GABA^g}$

Second glial glutamine pool

The addition of a second Gln pool was shown to describe more accurately the metabolic enrichment curves obtained upon ^{13}C-glucose administration in rats[2]. The authors proposed the existence of a non-visible Gln pool based on the difference in concentration observed between *in vivo* glutamine concentration measured with ^{1}H-MRS and *in vitro* with ^{1}H-NMR. The size of this second pool was proposed to be around half the total Gln concentration and in exchange with glial Gln only. As such, we used two distinct glial Gln pools of 50% (Gln^{g2}) and 30% (Gln^{g1}) of total Gln concentration. The addition of this pool led to an improvement in GlnC3(t) and GlnC4(t) enrichment fitting.

Gln pool 1: $\frac{dGln^{g1}{}_x}{dt} = V_{GS} \cdot \frac{Glu^g{}_x(t)}{Glu^g} - \left(V_{NT}{}^i + V_{NT}{}^e + V_{eff} + V_{ex}{}^g\right) \cdot \frac{Gln^{g1}{}_x(t)}{Gln^{g1}} + V_{ex}{}^g \frac{Gln^{g2}{}_x(t)}{Gln^{g2}}$

Gln pool 2: $\frac{dGln^{g2}{}_x}{dt} = V_{ex}{}^g \left(\frac{Gln^{g1}{}_x(t)}{Gln^{g1}} - \frac{Gln^{g2}{}_x(t)}{Gln^{g2}}\right)$

Second inhibitory GABA pool

With a comparable hypothesis of having two distinct metabolic pools of Gln in glia, we decided to include a second pool of GABA in inhibitory neurons. GABA is synthetized from glutamate decarboxylase (GAD) only in GABAergic neurons but by two different enzyme isoforms, and thus in two compartments[11]. GAD67, encoded by the gene *Gad1*, is expressed mainly in the cytoplasm of neurons and contributes to the "metabolic" GABA in neurons. GAD65, encoded by the gene *Gad2*, is located at the synapses and functionally regulated based on neurotransmission demand[12]. Relative GAD65 content in mouse hippocampus has been shown to be around 50% of total GAD[13]. Therefore, GABAergic GABA pools were divided in two equal pools.

GABA pool 1:

***GABA C2*:** $\frac{dGABA_2{}^{i1}}{dt} = V_{GAD} \cdot \frac{Glu_4{}^i(t)}{Glu^i} + V_{ex}{}^i \cdot \frac{GABA_2{}^{i2}(t)}{GABA^{i2}} - (V_{NT}{}^i + V_{shunt}{}^i + V_{ex}{}^i) \cdot \frac{GABA_2{}^{i1}(t)}{GABA^{i1}}$

***GABA C3*:** $\frac{dGABA_3{}^{i1}}{dt} = V_{GAD} \cdot \frac{Glu_3{}^i(t)}{Glu^i} + V_{ex}{}^i \cdot \frac{GABA_3{}^{i2}(t)}{GABA^{i2}} - (V_{NT}{}^i + V_{shunt}{}^i + V_{ex}{}^i) \cdot \frac{GABA_3{}^{i1}(t)}{GABA^{i1}}$

***GABA C4*:** $\frac{dGABA_4{}^{i1}}{dt} = V_{GAD} \cdot \frac{Glu_2{}^i(t)}{Glu^i} + V_{ex}{}^i \cdot \frac{GABA_4{}^{i2}(t)}{GABA^{i2}} - (V_{NT}{}^i + V_{shunt}{}^i + V_{ex}{}^i) \cdot \frac{GABA_4{}^{i1}(t)}{GABA^{i1}}$

GABA pool 2: $\frac{dGABA^{i2}{}_x}{dt} = V_{ex}{}^i \left(\frac{GABA^{i1}{}_x(t)}{GABA^{i1}} - \frac{GABA^{i2}{}_x(t)}{GABA^{i2}}\right)$

References

1. Lizarbe B, Lei H, Duarte JMN, et al. Feasibility of in vivo measurement of glucose metabolism in the mouse hypothalamus by 1H-[13C] MRS at 14.1T. *Magn Reson Med* 2018; 80: 874–884.

2. Duarte JMN, Gruetter R. Glutamatergic and GABAergic energy metabolism measured in the rat brain by 13 C NMR spectroscopy at 14.1 T. *J Neurochem* 2013; 126: 579–590.

3. Patel AB, de Graaf RA, Mason GF, et al. Glutamatergic Neurotransmission and Neuronal Glucose Oxidation are Coupled during Intense Neuronal Activation. *J Cereb Blood Flow Metab* 2004; 24: 972–985.

4. Boumezbeur F, Petersen KF, Cline GW, et al. The Contribution of Blood Lactate to Brain Energy Metabolism in Humans Measured by Dynamic 13C Nuclear Magnetic Resonance Spectroscopy. *J Neurosci* 2010; 30: 13983–13991.

5. Leong SF, Lai JC, Lim L, et al. Energy-metabolizing enzymes in brain regions of adult and aging rats. *J Neurochem* 1981; 37: 1548–56.

6. Xu S, Yang J, Shen J. In vivo13C saturation transfer effect of the lactate dehydrogenase reaction. *Magn Reson Med* 2007; 57: 258–264.

7. Gruetter R, Seaquist ER, Ugurbil K. A mathematical model of compartmentalized neurotransmitter metabolism in the human brain. *Am J Physiol Metab* 2001; 281: E100–E112.

8. Ottersen OP, Zhang N, Walberg F. Metabolic compartmentation of glutamate and glutamine: morphological evidence obtained by quantitative immunocytochemistry in rat cerebellum. *Neuroscience* 1992; 46: 519–34.

9. Bak LK, Schousboe A, Waagepetersen HS. The glutamate/GABA-glutamine cycle: aspects of transport, neurotransmitter homeostasis and ammonia transfer. *J Neurochem* 2006; 98: 641–653.

10. Lai M, Lanz B, Poitry-Yamate C, et al. In vivo 13 C MRS in the mouse brain at 14.1 Tesla and metabolic flux quantification under infusion of [1,6- 13 C 2]glucose. *J Cereb Blood Flow Metab* 2018; 38: 1701–1714.

11. Martin DL, Rimvall K. Regulation of gamma-Aminobutyric Acid Synthesis in the Brain. *J Neurochem* 1993; 60: 395–407.

12. Pinal CS, Tobin AJ. Uniqueness and redundancy in GABA production. *Perspect Dev Neurobiol* 1998; 5: 109–18.

13. Sheikh S., Martin S., Martin D. Regional distribution and relative amounts of glutamate decarboxylase isoforms in rat and mouse brain. *Neurochem Int* 1999; 35: 73–80.